US011653861B2

(12) **United States Patent**
Bechtel et al.

(10) **Patent No.: US 11,653,861 B2**
(45) **Date of Patent: May 23, 2023**

(54) **USING MONTE CARLO AND ITERATIVE TECHNIQUES TO DETERMINE TISSUE OXYGEN SATURATION**

(71) Applicant: **ViOptix, Inc.**, Newark, CA (US)

(72) Inventors: **Kate LeeAnn Bechtel**, Pleasant Hill, CA (US); **H. Keith Nishihara**, Los Altos, CA (US)

(73) Assignee: **ViOptix, Inc.**, Newark, CA (US)

(*) Notice: Subject to any disclaimer, the term of this patent is extended or adjusted under 35 U.S.C. 154(b) by 187 days.

(21) Appl. No.: **17/172,013**

(22) Filed: **Feb. 9, 2021**

(65) **Prior Publication Data**

US 2021/0161443 A1 Jun. 3, 2021

Related U.S. Application Data

(60) Division of application No. 15/820,368, filed on Nov. 21, 2017, now Pat. No. 10,912,503, which is a (Continued)

(51) **Int. Cl.**
A61B 5/1455 (2006.01)
A61B 90/00 (2016.01)
(Continued)

(52) **U.S. Cl.**
CPC ***A61B 5/14551*** (2013.01); ***A61B 5/0059*** (2013.01); ***A61B 5/0075*** (2013.01);
(Continued)

(58) **Field of Classification Search**
CPC A61B 5/1455; A61B 5/14552; A61B 5/14551; A61B 5/0059
See application file for complete search history.

(56) **References Cited**

U.S. PATENT DOCUMENTS

4,223,680 A 9/1980 Jobsis
4,286,599 A 9/1981 Hahn et al.
(Continued)

FOREIGN PATENT DOCUMENTS

JP 05-261088 10/1993
JP 10216115 A 8/1998
(Continued)

OTHER PUBLICATIONS

Hueber, Dennis et al., "New Optical Probe Designs for Absolute (Self-Calibrating) NIR Tissue Hemoglobin Measurements," in Proceedings of Optical Tomography and Spectroscopy of Tissue III, vol. 3597, 618-631(Jan. 1999).
(Continued)

Primary Examiner — Marjan Fardanesh
(74) *Attorney, Agent, or Firm* — Aka Chan LLP

(57) **ABSTRACT**

A method for determining oxygen saturation includes emitting light from sources into tissue; detecting the light by detectors subsequent to reflection; and generating reflectance data based on detecting the light. The method includes determining a first subset of simulated reflectance curves from a set of simulated reflectance curves stored in a tissue oximetry device for a coarse grid; and fitting the reflectance data points to the first subset of simulated reflectance curves to determine a closest fitting one of the simulated reflectance curves. The method includes determining a second subset of simulated reflectance curves for a fine grid based on the closest fitting one of the simulated reflectance curves; determining a peak of absorption and reflection coefficients from the fine grid; and determining an absorption and a reflectance coefficient for the reflectance data points by performing a weighted average of the absorption coefficients and reflection coefficients from the peak.

20 Claims, 8 Drawing Sheets

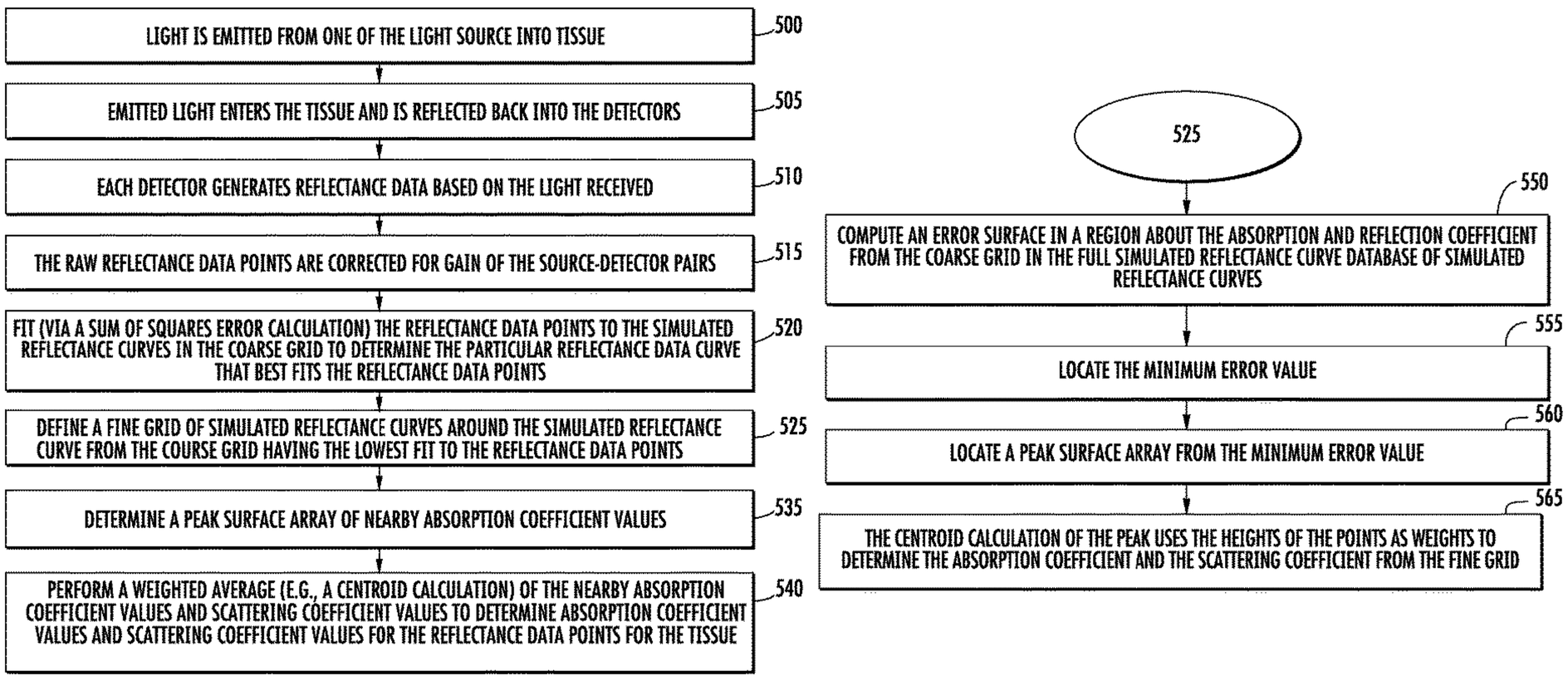

Related U.S. Application Data

division of application No. 15/163,565, filed on May 24, 2016, now Pat. No. 10,213,142, which is a continuation of application No. 13/887,220, filed on May 3, 2013, now Pat. No. 9,345,439.

(60) Provisional application No. 61/682,146, filed on Aug. 10, 2012, provisional application No. 61/642,399, filed on May 3, 2012, provisional application No. 61/642,395, filed on May 3, 2012, provisional application No. 61/642,389, filed on May 3, 2012, provisional application No. 61/642,393, filed on May 3, 2012.

(51) **Int. Cl.**

A61B 5/00	(2006.01)
A61B 5/1495	(2006.01)
A61M 35/00	(2006.01)
A61B 5/145	(2006.01)
A61B 90/11	(2016.01)
A61B 5/1459	(2006.01)
A61B 90/30	(2016.01)

(52) **U.S. Cl.**

CPC ***A61B 5/1455*** (2013.01); ***A61B 5/1459*** (2013.01); ***A61B 5/1495*** (2013.01); ***A61B 5/14546*** (2013.01); ***A61B 5/14552*** (2013.01); ***A61B 5/72*** (2013.01); ***A61B 5/7246*** (2013.01); ***A61B 5/7282*** (2013.01); ***A61B 5/74*** (2013.01); ***A61B 5/742*** (2013.01); ***A61B 5/7405*** (2013.01); ***A61B 5/7475*** (2013.01); ***A61B 90/11*** (2016.02); ***A61B 90/39*** (2016.02); ***A61M 35/003*** (2013.01); *A61B 2090/065* (2016.02); *A61B 2090/306* (2016.02); *A61B 2090/395* (2016.02); *A61B 2560/0431* (2013.01); *A61B 2560/0475* (2013.01); *A61B 2562/0271* (2013.01); *A61B 2562/166* (2013.01)

(56) **References Cited**

U.S. PATENT DOCUMENTS

5,088,493	A	2/1992	Giannini et al.
5,218,962	A	6/1993	Mannheimer et al.
5,517,301	A	5/1996	Dave
5,517,987	A	5/1996	Tsuchiya
5,690,113	A	11/1997	Sliwa, Jr et al.
6,056,692	A	5/2000	Schwartz
6,070,093	A	5/2000	Oosta et al.
6,078,833	A	6/2000	Hueber
6,197,034	B1	3/2001	Gvozdic et al.
6,285,904	B1	9/2001	Weber et al.
6,453,183	B1	9/2002	Walker
6,516,209	B2	2/2003	Cheng et al.
6,549,284	B1	4/2003	Boas et al.
6,587,701	B1	7/2003	Stranc et al.
6,587,703	B2	7/2003	Cheng et al.
6,597,931	B1	7/2003	Cheng et al.
6,708,048	B1	3/2004	Chance
6,735,458	B2	5/2004	Cheng et al.
6,766,188	B2	7/2004	Soller
6,839,580	B2	1/2005	Zonios et al.
7,247,142	B1	7/2007	Elmandjra et al.
7,254,427	B2	8/2007	Cho et al.
7,344,587	B2	3/2008	Kahn et al.
D567,949	S	4/2008	Lash et al.
7,355,688	B2	4/2008	Lash et al.
D568,479	S	5/2008	Mao et al.
7,657,293	B2	2/2010	Lash et al.
8,798,700	B1	8/2014	Heaton et al.
2002/0019587	A1	2/2002	Cheng et al.
2002/0179094	A1	12/2002	Perlow
2004/0111016	A1	6/2004	Casscells et al.
2004/0260161	A1	12/2004	Melker
2005/0177069	A1	8/2005	Takizawa et al.
2005/0250998	A1	11/2005	Huiku
2005/0277818	A1	12/2005	Myers
2006/0129037	A1	6/2006	Kaufman et al.
2007/0149886	A1	6/2007	Kohls
2008/0015422	A1	1/2008	Wessel
2008/0015424	A1	1/2008	Bernreuter
2008/0139908	A1	6/2008	Kurth
2008/0181715	A1	7/2008	Cohen
2005/0319290		12/2008	Mao et al.
2008/0319290	A1	12/2008	Mao et al.
2009/0234209	A1	9/2009	Lash et al.
2009/0275805	A1	11/2009	Lane et al.
2010/0010486	A1	1/2010	Mehta et al.
2011/0028814	A1	2/2011	Petersen et al.
2011/0046458	A1	2/2011	Pinedo et al.
2011/0205535	A1	8/2011	Soller et al.
2011/0224518	A1	9/2011	Tindi et al.
2011/0237911	A1	9/2011	Lamego et al.

FOREIGN PATENT DOCUMENTS

JP	11244268 A	12/1999
JP	2006109964	4/2006
KR	1020000075056	12/2000
KR	10-2009-0016744	2/2009
KR	1020090016744	2/2009
WO	2011008382	1/2011

OTHER PUBLICATIONS

Mittnacht, et al., "Methylene Blue Administration is Associated with Decreased Cerebral Oximetry Values," Anesthesia & Analgesia, Aug. 2008, vol. 105, No. 2, pp. 549-550.

Alexandrakis, et al., "Accuracy of the Diffusion Approximation in Determining the Optical Properties of a Two-Layer Turbid Medium," Applied Optics, vol. 37, No. 31, Nov. 1, 1998, pp. 7403-7409.

Cen, et al., "Optimization of Inverse Algorithm for Estimating the Optical Properties of Biological Materials Using Spatially-Resolved Diffuse Reflectance," Inverse Problems in Science and Engineering, vol. 18, No. 6, Sep. 2010, pp. 853-872.

Dam, et al., "Determination of Tissue Optical Properties from Diffuse Reflectance Profiles by Multivariate Calibration," Applied Optics, vol. 37, No. 4, Feb. 1, 1998, pp. 772-778.

Farrell, et al., "Influence of Layered Tissue Architecture on Estimates of Tissue Optical Properties Obtained from Spatially Resolved Diffuse Reflectometry," Applied Optics, vol. 37, No. 10, Apr. 1, 1998, pp. 1958-1972.

Fawzi, et al., "Determination of the Optical Properties of a Two-Layer Tissue Model by Detecting Photons Migrating at Progressively Increasing Depths," Applied Optics, vol. 42, No. 31, Nov. 1, 2003, pp. 6398-6411.

Kienle, et al., "Spatially Resolved Absolute Diffuse Reflectance Measurements for Noninvasive Determination of the Optical Scattering and Absorption Coefficients of Biological Tissue," Applied Optics, vol. 35, No. 13, May 1, 1996, pp. 2304-2314.

Nichols, et al., "Design and Testing of a White-Light, Steady-State Diffuse Reflectance Spectrometer for Determination of Optical Properties of Highly Scattering Systems," Applied Optics, vol. 36, No. 1, Jan. 1, 1997, pp. 93-104.

Seo, et al., "Perturbation and Differential Monte Carlo Methods for Measurement of Optical Properties in a Layered Epithelial Tissue Model," Journal of Biomedical Optics, vol. 12(1), 014030, Jan./Feb. 2007, pp. 1-15.

Tseng, et al., "In Vivo Determination of Skin Near-Infrared Optical Properties Using Diffuse Optical Spectroscopy," Journal of Biomedical Optics, vol. 13(1), 014016, Jan./Feb. 2008, pp. 1-7.

Tseng, et al., "Analysis of a Diffusion-Model-Based Approach for Efficient Quantification of Superficial Tissue Properties," Optics Letters, vol. 35, No. 22, Nov. 15, 2010, pp. 3739-3741.

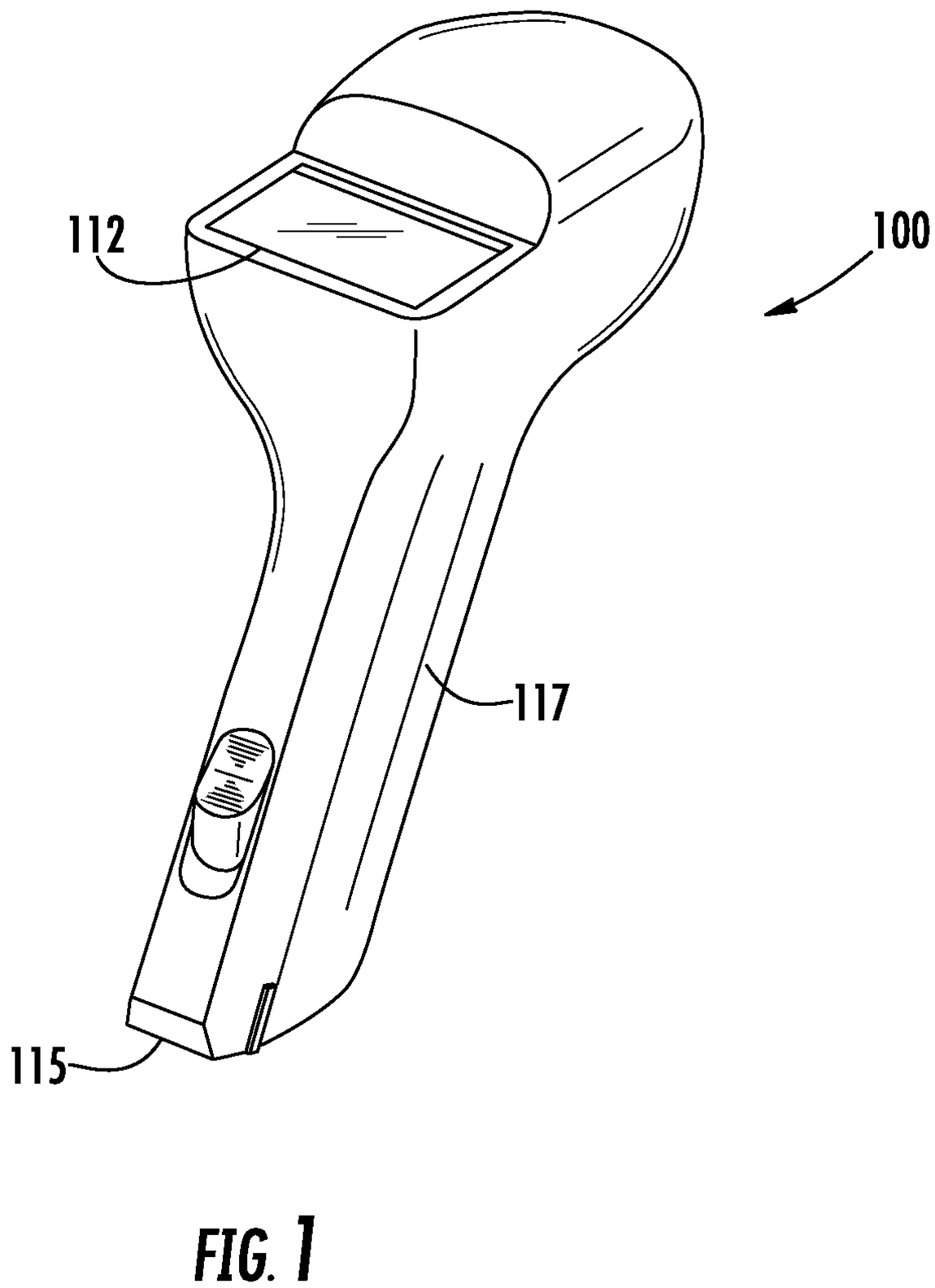

FIG. 1

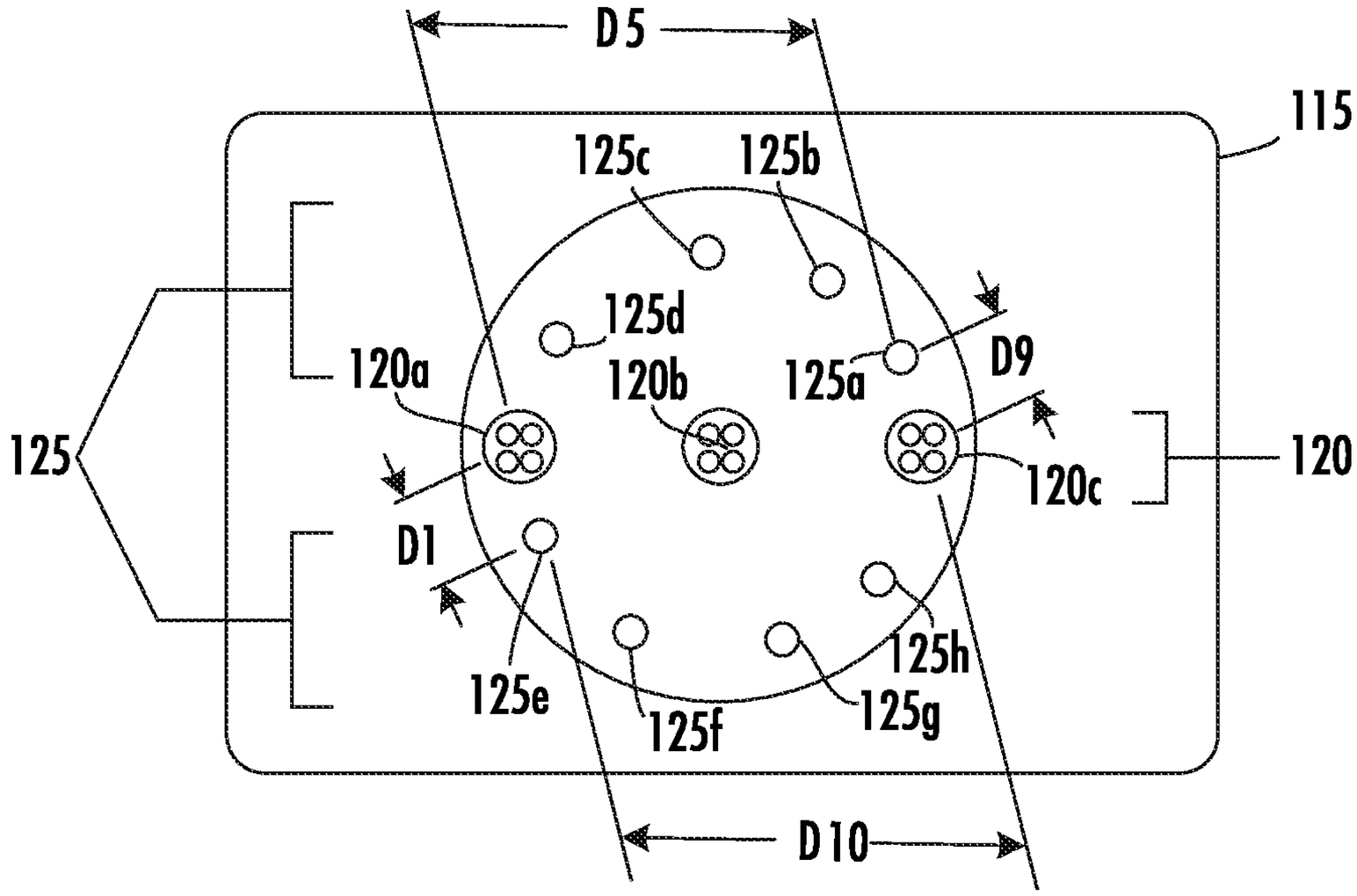
D5
115
125c
125b
125d
120a
120b
125a
D9
125
120
120c
D1
125e
125f
125g
125h
D10

FIG. 2A

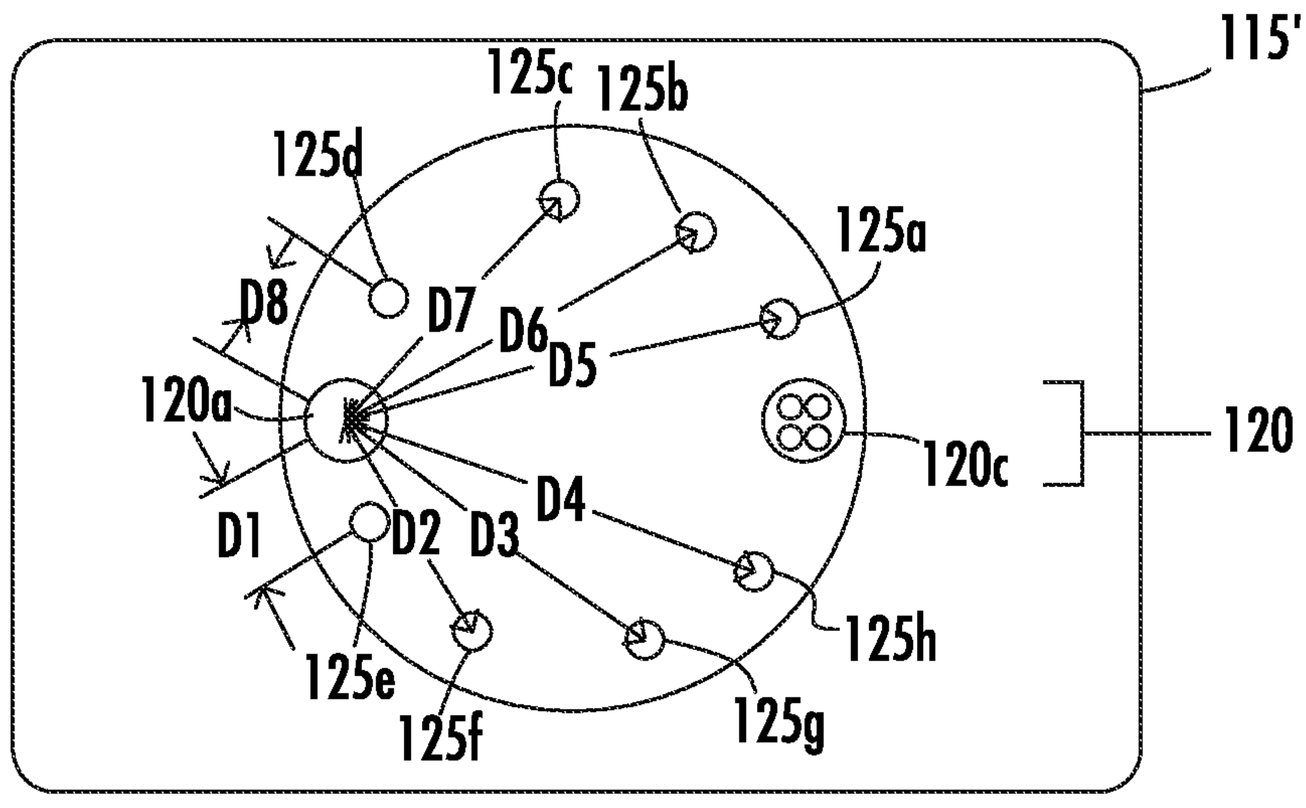
115'
125c
125b
125d
125a
D8
D7
D6
D5
120a
120c
120
D4
D1
D2
D3
125h
125e
125f
125g

FIG. 2B

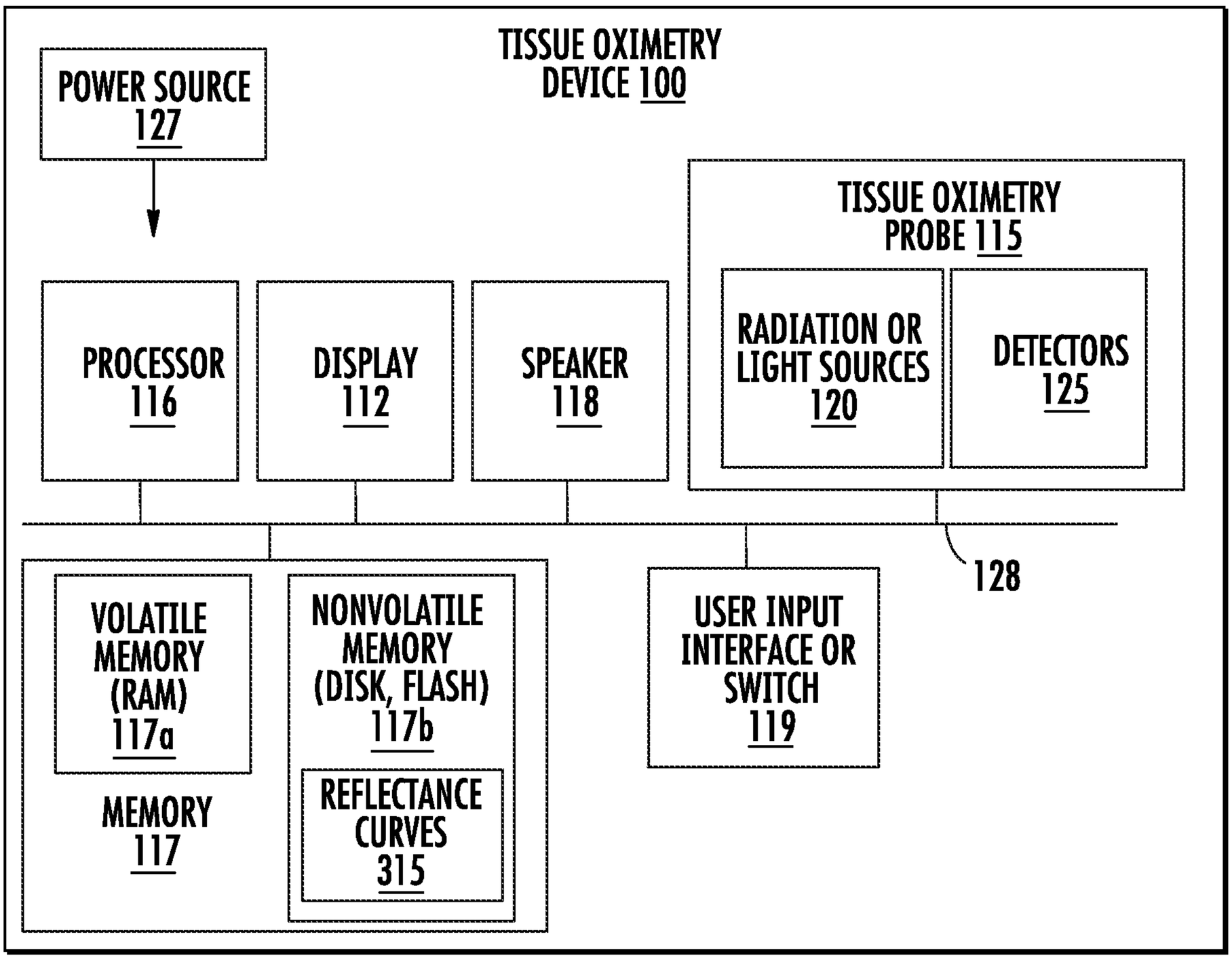
TISSUE OXIMETRY DEVICE 100
POWER SOURCE 127
TISSUE OXIMETRY PROBE 115
PROCESSOR 116
DISPLAY 112
SPEAKER 118
RADIATION OR LIGHT SOURCES 120
DETECTORS 125
128
VOLATILE MEMORY (RAM) 117a
NONVOLATILE MEMORY (DISK, FLASH) 117b
REFLECTANCE CURVES 315
MEMORY 117
USER INPUT INTERFACE OR SWITCH 119

FIG. 3

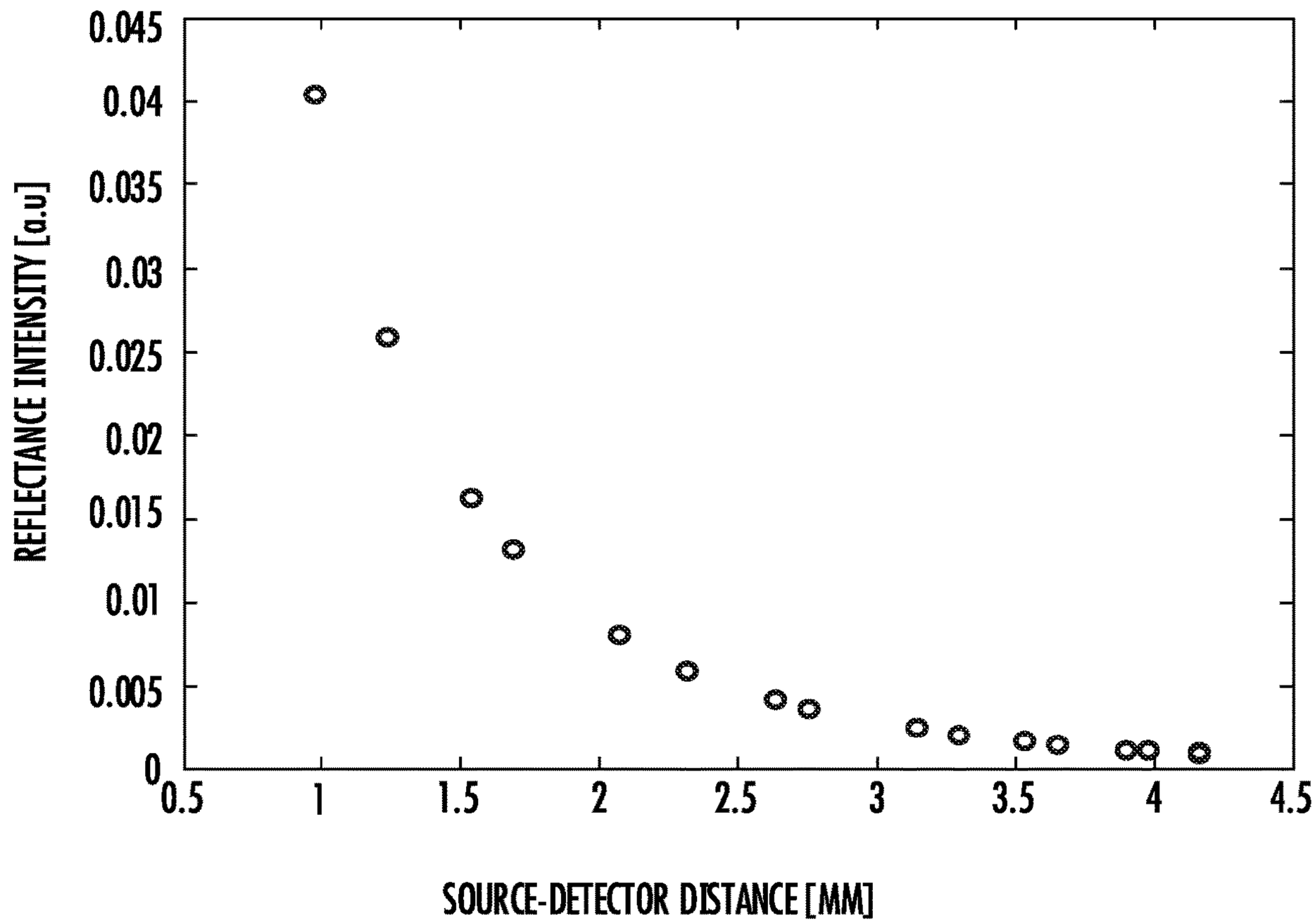
0.045
0.04
0.035
0.03
0.025
0.02
0.015
0.01
0.005
0
REFLECTANCE INTENSITY [a.u]
0.5
1
1.5
2
2.5
3
3.5
4
4.5
SOURCE-DETECTOR DISTANCE [MM]

FIG. 4

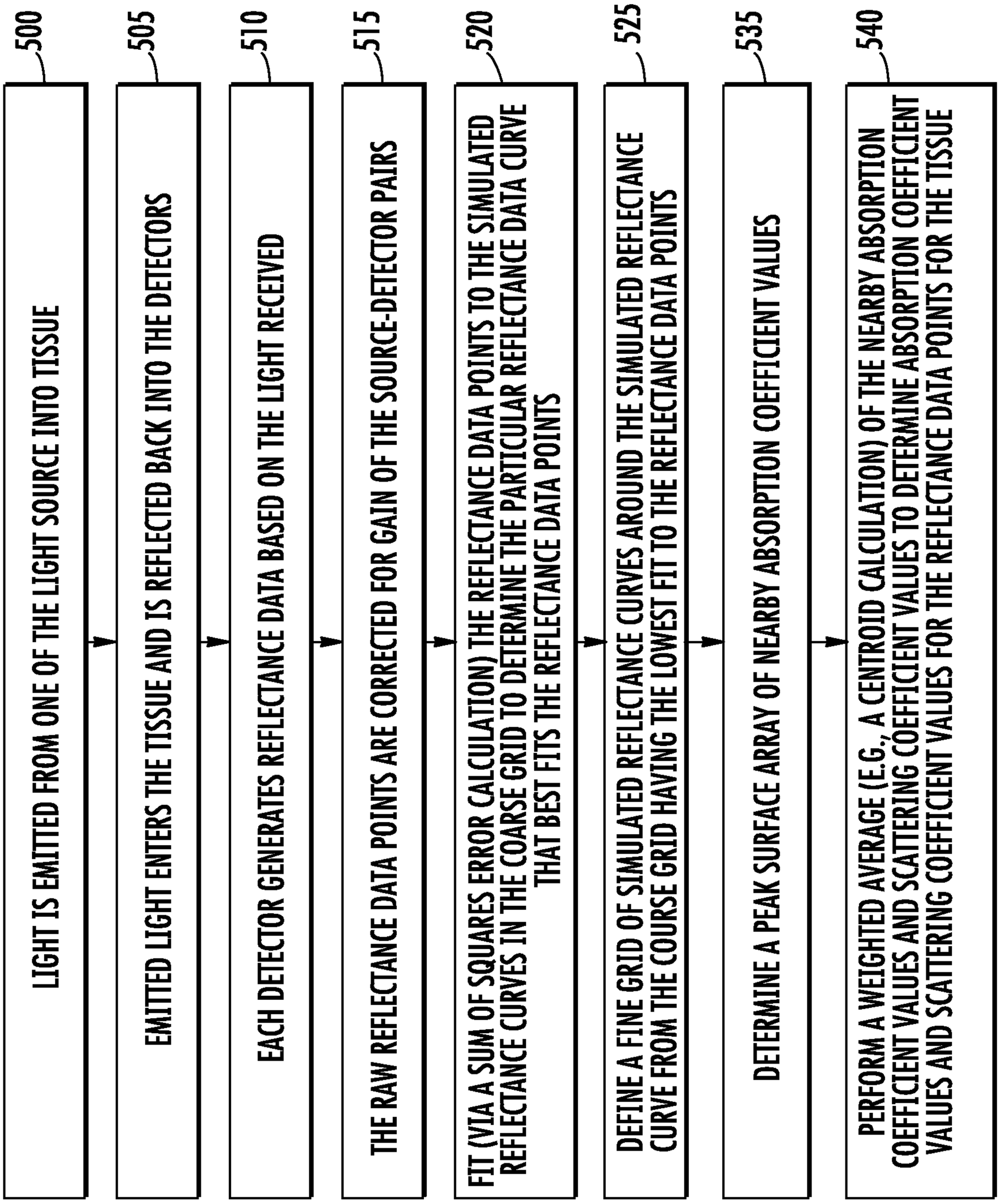
500
LIGHT IS EMITTED FROM ONE OF THE LIGHT SOURCE INTO TISSUE
505
EMITTED LIGHT ENTERS THE TISSUE AND IS REFLECTED BACK INTO TO THE DETECTORS
510
EACH DETECTOR GENERATES REFLECTANCE DATA BASED ON THE LIGHT RECEIVED
515
THE RAW REFLECTANCE DATA POINTS ARE CORRECTED FOR GAIN OF THE SOURCE-DETECTOR PAIRS
520
FIT (VIA A SUM OF SQUARES ERROR CALCULATION) THE REFLECTANCE DATA POINTS TO THE SIMULATED REFLECTANCE CURVES IN THE COARSE GRID TO DETERMINE THE PARTICULAR REFLECTANCE DATA CURVE THAT BEST FITS THE REFLECTANCE DATA POINTS
525
DEFINE A FINE GRID OF SIMULATED REFLECTANCE CURVES AROUND THE SIMULATED REFLECTANCE DATA CURVE FROM THE COURSE GRID HAVING THE LOWEST FIT TO THE REFLECTANCE DATA POINTS
535
DETERMINE A PEAK SURFACE ARRAY OF NEARBY ABSORPTION COEFFICIENT VALUES
540
PERFORM A WEIGHTED AVERAGE (E.G., A CENTROID CALCULATION) OF THE NEARBY ABSORPTION COEFFICIENT VALUES AND SCATTERING COEFFICIENT VALUES TO DETERMINE ABSORPTION COEFFICIENT VALUES FOR THE REFLECTANCE DATA POINTS FOR THE TISSUE

FIG. 5A

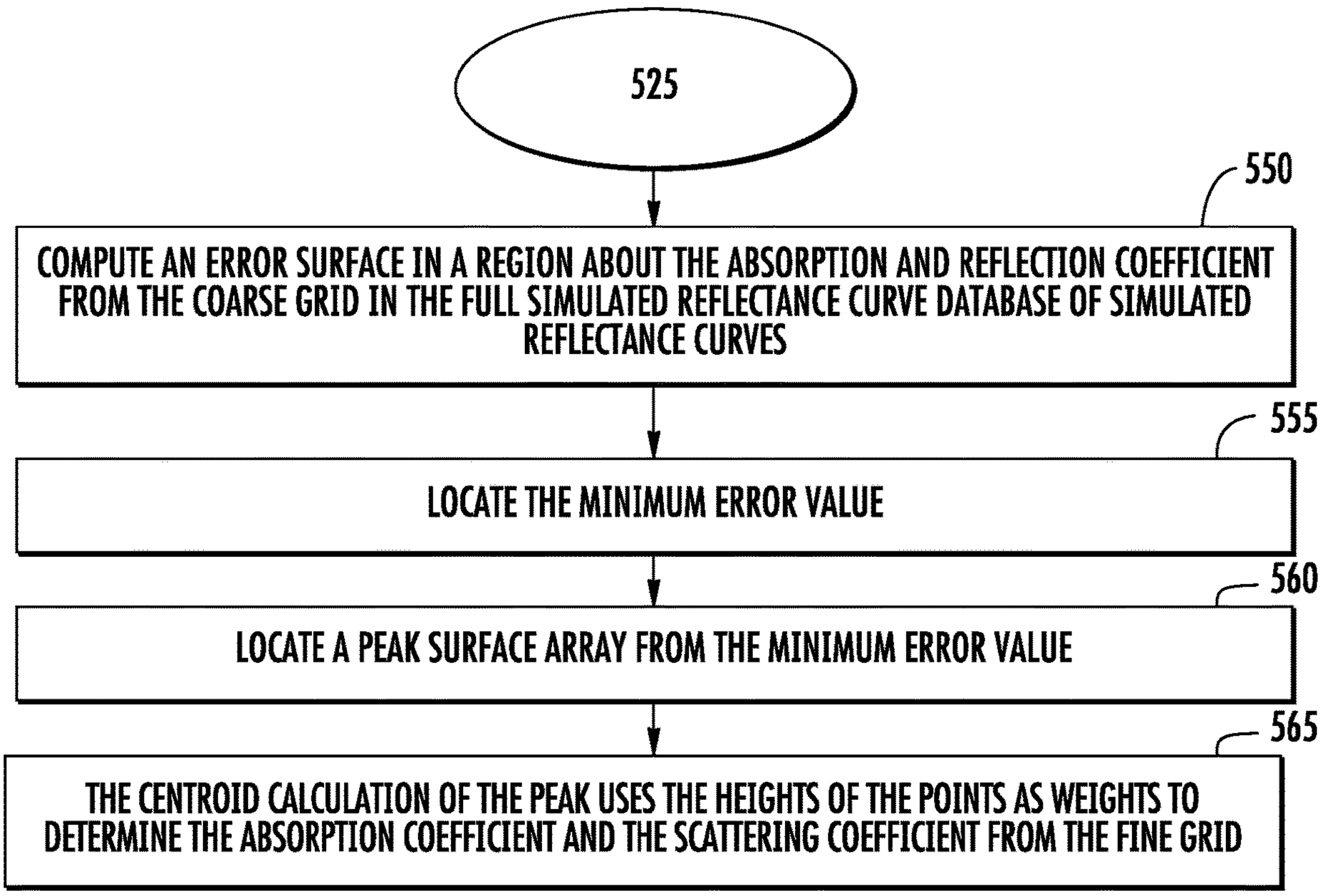
525
550
COMPUTE AN ERROR SURFACE IN A REGION ABOUT THE ABSORPTION AND REFLECTION COEFFICIENT FROM THE COARSE GRID IN THE FULL SIMULATED REFLECTANCE CURVE DATABASE OF SIMULATED REFLECTANCE CURVES
555
LOCATE THE MINIMUM ERROR VALUE
560
LOCATE A PEAK SURFACE ARRAY FROM THE MINIMUM ERROR VALUE
565
THE CENTROID CALCULATION OF THE PEAK USES THE HEIGHTS OF THE POINTS AS WEIGHTS TO DETERMINE THE ABSORPTION COEFFICIENT AND THE SCATTERING COEFFICIENT FROM THE FINE GRID

FIG. 5B

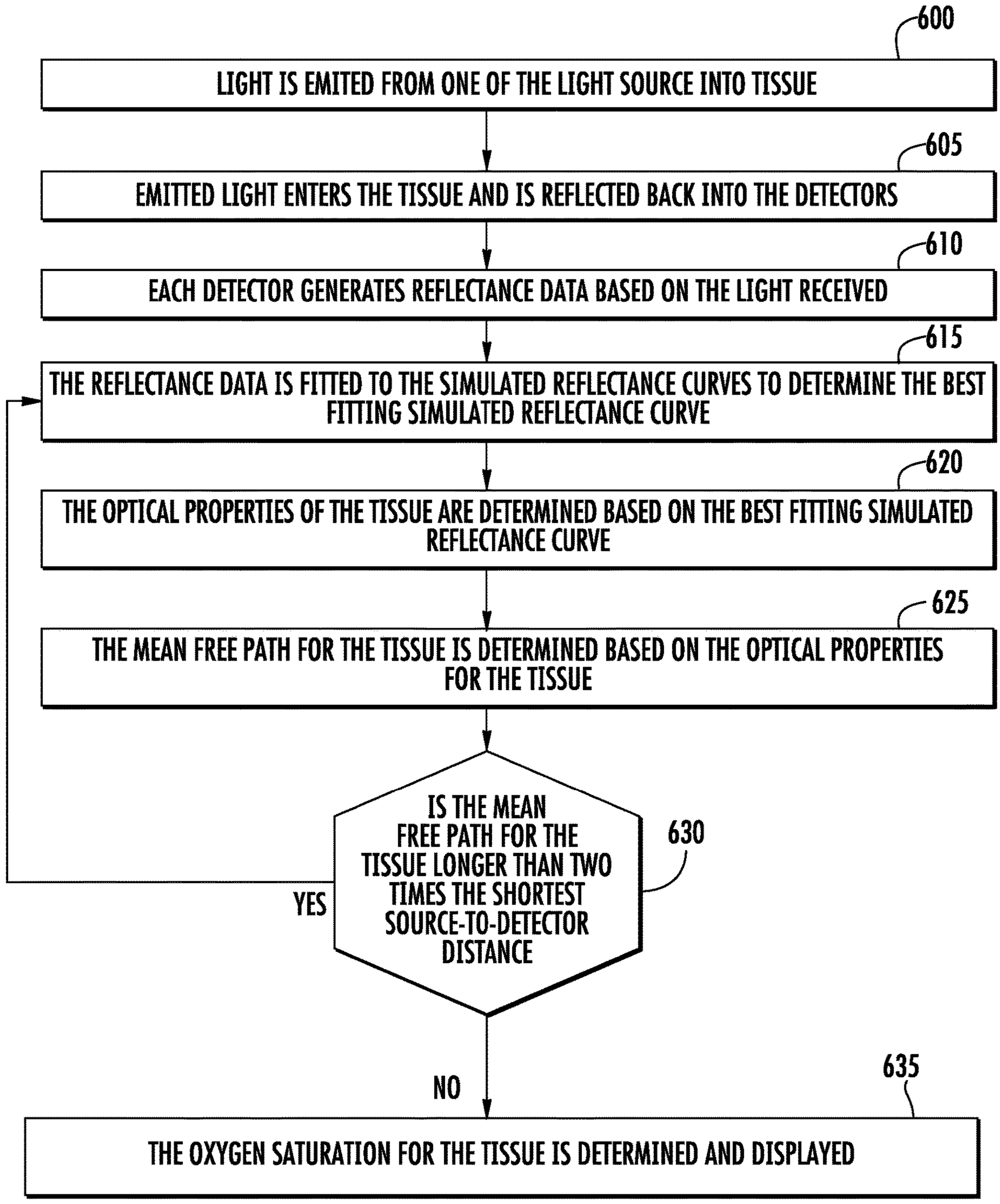
600
LIGHT IS EMITED FROM ONE OF THE LIGHT SOURCE INTO TISSUE
605
EMITTED LIGHT ENTERS THE TISSUE AND IS REFLECTED BACK INTO THE DETECTORS
610
EACH DETECTOR GENERATES REFLECTANCE DATA BASED ON THE LIGHT RECEIVED
615
THE REFLECTANCE DATA IS FITTED TO THE SIMULATED REFLECTANCE CURVES TO DETERMINE THE BEST FITTING SIMULATED REFLECTANCE CURVE
620
THE OPTICAL PROPERTIES OF THE TISSUE ARE DETERMINED BASED ON THE BEST FITTING SIMULATED REFLECTANCE CURVE
625
THE MEAN FREE PATH FOR THE TISSUE IS DETERMINED BASED ON THE OPTICAL PROPERTIES FOR THE TISSUE
IS THE MEAN FREE PATH FOR THE TISSUE LONGER THAN TWO TIMES THE SHORTEST SOURCE-TO-DETECTOR DISTANCE
630
YES
NO
635
THE OXYGEN SATURATION FOR THE TISSUE IS DETERMINED AND DISPLAYED

FIG. 6

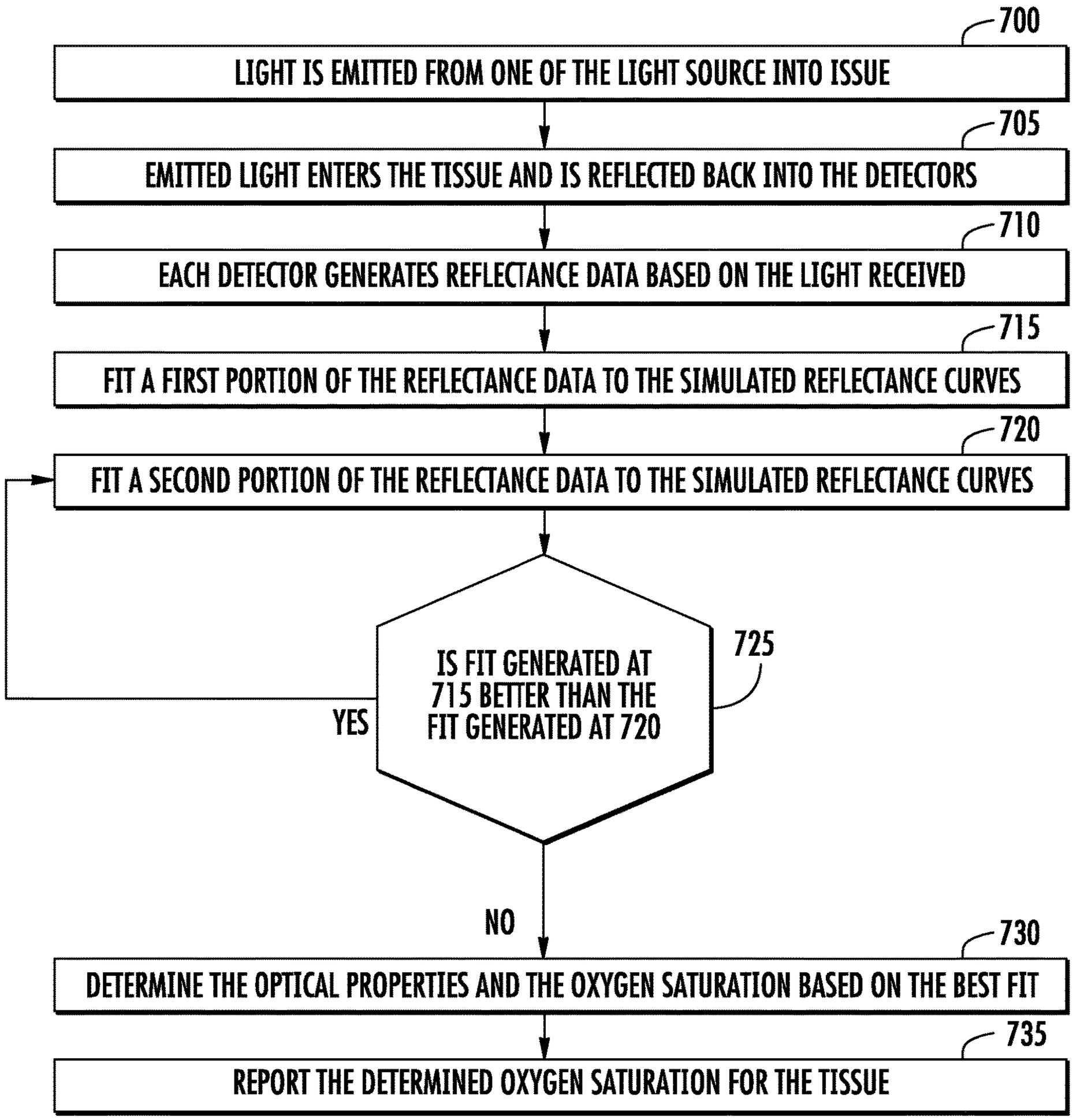
700
LIGHT IS EMITTED FROM ONE OF THE LIGHT SOURCE INTO ISSUE
705
EMITTED LIGHT ENTERS THE TISSUE AND IS REFLECTED BACK INTO THE DETECTORS
710
EACH DETECTOR GENERATES REFLECTANCE DATA BASED ON THE LIGHT RECEIVED
715
FIT A FIRST PORTION OF THE REFLECTANCE DATA TO THE SIMULATED REFLECTANCE CURVES
720
FIT A SECOND PORTION OF THE REFLECTANCE DATA TO THE SIMULATED REFLECTANCE CURVES
IS FIT GENERATED AT 715 BETTER THAN THE FIT GENERATED AT 720
725
YES
NO
730
DETERMINE THE OPTICAL PROPERTIES AND THE OXYGEN SATURATION BASED ON THE BEST FIT
735
REPORT THE DETERMINED OXYGEN SATURATION FOR THE TISSUE

FIG. 7

USING MONTE CARLO AND ITERATIVE TECHNIQUES TO DETERMINE TISSUE OXYGEN SATURATION

CROSS-REFERENCE TO RELATED APPLICATIONS

This patent application is a divisional of U.S. patent application Ser. No. 15/820,368, filed Nov. 21, 2017, issued as U.S. Pat. No. 10,912,503 on Feb. 9, 2021, which is a divisional of U.S. patent application Ser. No. 15/163,565, filed May 24, 2016, issued as U.S. Pat. No. 10,213,142 on Feb. 26, 2019, which is a continuation of U.S. patent application Ser. No. 13/887,220, filed May 3, 2013, issued as U.S. Pat. No. 9,345,439 on May 24, 2016, which claims the benefit of U.S. patent applications 61/642,389, 61/642,393, 61/642,395, and 61/642,399, filed May 3, 2012, and 61/682,146, filed Aug. 10, 2012. These applications are incorporated by reference along with all other references cited in this application.

BACKGROUND OF THE INVENTION

The present invention relates generally to optical systems that monitor oxygen levels in tissue. More specifically, the present invention relates to optical probes, such as oximeters, that include sources and detectors on sensor heads of the optical probes and that use locally stored simulated reflectance curves for determining oxygen saturation of tissue.

Oximeters are medical devices used to measure oxygen saturation of tissue in humans and living things for various purposes. For example, oximeters are used for medical and diagnostic purposes in hospitals and other medical facilities (e.g., surgery, patient monitoring, or ambulance or other mobile monitoring for, e.g., hypoxia); sports and athletics purposes at a sports arena (e.g., professional athlete monitoring); personal or at-home monitoring of individuals (e.g., general health monitoring, or person training for a marathon); and veterinary purposes (e.g., animal monitoring).

Pulse oximeters and tissue oximeters are two types of oximeters that operate on different principles. A pulse oximeter requires a pulse in order to function. A pulse oximeter typically measures the absorbance of light due to the pulsing arterial blood. In contrast, a tissue oximeter does not require a pulse in order to function, and can be used to make oxygen saturation measurements of a tissue flap that has been disconnected from a blood supply.

Human tissue, as an example, includes a variety of light-absorbing molecules. Such chromophores include oxygenated and deoxygenated hemoglobins, melanin, water, lipid, and cytochrome. Oxygenated and deoxygenated hemoglobins are the most dominant chromophores in tissue for much of the visible and near-infrared spectral range. Light absorption differs significantly for oxygenated and deoxygenated hemoglobins at certain wavelengths of light. Tissue oximeters can measure oxygen levels in human tissue by exploiting these light-absorption differences.

Despite the success of existing oximeters, there is a continuing desire to improve oximeters by, for example, improving measurement accuracy; reducing measurement time; lowering cost; reducing size, weight, or form factor; reducing power consumption; and for other reasons, and any combination of these.

In particular, assessing a patient's oxygenation state, at both the regional and local level, is important as it is an indicator of the state of the patient's health. Thus, oximeters

are often used in clinical settings, such as during surgery and recovery, where it may be suspected that the patient's tissue oxygenation state is unstable. For example, during surgery, oximeters should be able to quickly deliver accurate oxygen saturation measurements under a variety of non-ideal conditions. While existing oximeters have been sufficient for post-operative tissue monitoring where absolute accuracy is not critical and trending data alone is sufficient, accuracy is, however, required during surgery in which spot-checking can be used to determine whether tissue might remain viable or needs to be removed.

Therefore, there is a need for an improved tissue oximetry probes and methods of making measurements using these probes.

BRIEF SUMMARY OF THE INVENTION

A tissue oximetry device utilizes a relatively large number of simulated reflectance curves to quickly determine the optical properties of tissue under investigation. The optical properties of the tissue allow for the further determination of the oxygenated hemoglobin and deoxygenated hemoglobin concentrations of the tissue as well as the oxygen saturation of the tissue.

According to a specific embodiment, a method for determining oxygen saturation of tissue via a tissue oximetry device includes emitting light from a set of light sources into tissue; detecting the light by a plurality of detectors subsequent to reflection of the light from the tissue; and generating reflectance data points for the tissue based on detecting the light by the plurality of detectors. The method further includes determining a first subset of simulated reflectance curves from a set of simulated reflectance curves stored in the tissue oximetry device for a coarse grid; and fitting the reflectance data points to the first subset of simulated reflectance curves included in the coarse grid to determine a closest fitting one of the simulated reflectance curves included in the coarse grid. The method further includes determining a second subset of simulated reflectance curves from the set of simulated reflectance curves stored in the tissue oximetry device for a fine grid based on the closest fitting one of the simulated reflectance curves included in the coarse grid. The method further includes determining a peak surface array of absorption coefficients and reflection coefficients from the fine grid; and determining an absorption coefficient and a reflectance coefficient for the reflectance data points by performing a weighted average of the absorption coefficients and reflection coefficients from the peak surface array. The weighted average may be a centroid calculation.

According to a specific implementation of the method, fitting the reflectance data points to a subset of simulated reflectance curves included in the coarse grid includes calculating a sum of squares error between the reflectance data points and each of the simulated reflectance curves of the coarse grid. According to another specific embodiment of the method, fitting the reflectance data points to a subset of simulated reflectance curves included in the fine grid includes calculating a sum of squares error between the reflectance data points and each of the simulated reflectance curves of the fine grid.

According to a specific implementation, the method further includes determining an oxygen saturation value for the tissue based on the scattering coefficient and the absorption coefficients for the tissue. Determining the oxygen saturation includes generating a look-up table of oxygen saturation values for finding a best fit of absorption coefficients based

on a range of probable total hemoglobin, melanin, and oxygen saturation values. Determining the oxygen saturation may further include converting the absorption coefficients to a unit vector; dividing the unit vector by a norm of the unit vector to reduce systematic error; and comparing the unit vector to the look-up table to find a best fit of the unit vector to the oxygen saturations of the look-up table.

According to another embodiment, a tissue oximetry device includes a processor; a memory storing a plurality of simulated reflectance curves; a light source configured to be controlled by the processor; and a plurality of detectors configured to be controlled by the processor; wherein the processor is configured to: control the light source to emit light into tissue; control the detectors to detect the light subsequent to reflection of the light from the tissue; control the detectors to generate reflectance data based on detecting the light; determine a first subset of simulated reflectance curves from a set of simulated reflectance curves stored in the tissue oximetry device for a coarse grid; fit the reflectance data points to the first subset of simulated reflectance curves included in the coarse grid to determine a closest fitting one of the simulated reflectance curves included in the coarse grid; determine a second subset of simulated reflectance curves from the set of simulated reflectance curves stored in the tissue oximetry device for a fine grid based on the closest fitting one of the simulated reflectance curves included in the coarse grid; and fit the reflectance data points to the second subset of simulated reflectance curves included in the fine grid to determine a closest fitting one of the simulated reflectance curves included in the fine grid, wherein one of the simulated reflectance curve from the fine grid that closest fits the reflectance data points represents a scattering coefficient and an absorption coefficient for the tissue.

In one implementation, the tissue oximetry device can measure oxygen saturation without requiring a pulse or heart beat. A tissue oximetry device of the invention is applicable to many areas of medicine and surgery including plastic surgery. The tissue oximetry device can make oxygen saturation measurements of tissue where there is no pulse. Such tissue may have been separated from the body (e.g., a flap) and will be transplanted to another place in the body. Aspects of the invention may also be applicable to a pulse oximeter. In contrast to a tissue oximetry device, a pulse oximeter requires a pulse in order to function. A pulse oximeter typically measures the absorbance of light due to the pulsing arterial blood.

Other objects, features, and advantages of the present invention will become apparent upon consideration of the following detailed description and the accompanying drawings, in which like reference designations represent like features throughout the figures.

BRIEF DESCRIPTION OF THE DRAWINGS

FIG. **1** is a simplified image of a tissue oximetry device according to one embodiment.

FIGS. **2**A and **2**B are simplified end views of a tissue oximetry probe of the tissue oximetry device according to a pair of alternative embodiments.

FIG. **3** is a block diagram of the tissue oximetry device according to one embodiment.

FIG. **4** is an example graph of a number of Monte Carlo-simulated reflectance curves.

FIG. **5**A is a high-level flow diagram of a method for determining the optical properties of tissue (e.g., real tissue) by tissue oximetry device where the tissue oximetry device uses reflectance data and simulated reflectance curves to determine the optical properties.

FIG. **5**B is a high-level flow diagram of a method for finding the particular simulated reflectance curve that best bits the reflectance data points in the fine grid according to one implementation.

FIG. **6** is a high-level flow diagram of another method for determining the optical properties and tissue properties of real tissue by the tissue oximetry device.

FIG. **7** is a high-level flow diagram of a method for weighting reflectance data generated by select detectors.

DETAILED DESCRIPTION OF THE INVENTION

FIG. **1** is a simplified image of a tissue oximetry device **100** according to one embodiment. Tissue oximetry device **100** is configured to make tissue oximetry measurements, such as intraoperatively and postoperatively. Tissue oximetry device **100** may be a handheld device that includes a tissue oximetry probe **115** (also referred to as a sensor head), which may be positioned at an end of a sensing arm **117**. Tissue oximetry device **100** is configured to measure the oxygen saturation of tissue by emitting light, such as near-infrared light, from tissue oximetry probe **115** into tissue, and collecting light reflected from the tissue at the tissue oximetry probe.

Tissue oximetry device **100** may include a display **112** or other notification device that notifies a user of oxygen saturation measurements made by the tissue oximetry device. While tissue oximetry probe **115** is described as being configured for use with tissue oximetry device **100**, which is a handheld device, tissue oximetry probe **115** may be used with other tissue oximetry devices, such as a modular tissue oximetry device where the tissue oximetry probe is at the end of a cable device that couples to a base unit. The cable device might be a disposable device that is configured for use with one patient and the base unit might be a device that is configured for repeated use. Such modular tissue oximetry devices are well understood by those of skill in the art and are not described further.

FIG. **2**A is a simplified end view of tissue oximetry probe **115** according to one embodiment. Tissue oximetry probe **115** is configured to contact tissue (e.g., a patient's skin) for which a tissue oximetry measurement is to be made. Tissue oximetry probe **115** includes a set of light sources **120** (generally light sources **120**) and includes a set of detectors **125** (generally detectors **125**). The set of light sources **120** may include two or more light sources. According to the embodiment shown in FIG. **2**A, tissue oximetry probe **115** includes three light sources **120***a*, **120***b*, and **120***c*, but may alternatively include two light sources, such as light sources **120***a* and **120***c* where light source **120***b* is omitted. Additional light sources (not shown) can be added. FIG. **2**B is a simplified end view of a tissue oximetry probe **115'** according to an embodiment where the tissue oximetry probe includes the two light sources **120***a* and **120***c*, but does not include light source **120***b*. Aside from the different number of light sources, tissue oximetry probes **115** and **115'** are substantially similar.

The set of detectors **125** may include eight detectors **125***a*, **125***b*, **125***c*, **125***d*, **125***e*, **125***f*, **125***g*, and **125***h* as shown, but may include more or fewer detectors. Detectors **125** are positioned with respect to outer light sources **120***a* and **120***c* such that eight or more (e.g., fourteen) unique source-to-detector distances are created. The shortest source-to-detector distances may be the same. For example, the shortest

source-to-detector distance D1 between light source **120***a* and detector **125***e*, and the shortest source-to-detector distance D9 between light source **120***c* and detector **125***a* may be the same. It follows that the source-to-detector distance D5 between light source **120***a* and detector **125***a*, and the source-to-detector distance D10 between light source **120***c* and detector **125***e* may also be the same. The source-to-detector distances D5 and D10 are the longest source-to-detector distance for light sources **120***a* and **120***c*.

With the exception of the shortest source-to-detector distance and the longest source-to-detector distance for light sources **120***a* and **120***c*, the source-to-detector distances for light sources **120***a* and **120***c* may be unique. As described above, tissue oximetry probe **115** may have fourteen unique source-to-detector distances that allow for fourteen reflectance data points to be collected by detectors **125** from light emitted from light sources **120***a* and **120***c*.

Furthermore, the source-to-detector distances for light sources **120***a* and **120***c* may also be selected such that the increases in the distances are substantially uniform. Thereby, a plot of source-to-detector distance verses reflectance detected by detectors **125** can provide a reflectance curve where the data points are well spaced along the x-axis. These spacings of the distances between light sources **120***a* and **120***c*, and detectors **125** reduces data redundancy and can lead to the generation of relatively accurate reflectance curves (further described below).

While the tissue oximetry probes **115** and **115'** described above have circularly arranged detectors, the detectors may be positioned in other arrangements, such as randomly, triangular, rectangular, square, ovoid, or the like. In some embodiments, the light sources may also be alternatively arranged, such as randomly, in triangular, rectangular, ovoid, or other shapes.

FIG. **3** is a block diagram of tissue oximetry device **100** according to one embodiment. Tissue oximetry device **100** includes display **112**, a processor **116**, a memory **117**, a speaker **118**, one or more user-selection devices **119** (e.g., one or more switches), a set of light sources **120**, a set of detectors **125**, and a power source (e.g., a battery) **127**. The foregoing listed components may be linked together via a bus **128**, which may be the system bus architecture of tissue oximetry device **100**. Although this figure shows one bus that connects to each component, the busing is illustrative of any interconnection scheme serving to link these components or other components included in tissue oximetry device **100** subsystems. For example, speaker **118** could be connected to a subsystem through a port or have an internal direct connection to processor **116**. Further, the components described are housed in a mobile housing (see FIG. **1**) of tissue oximetry device **100** according to at least one embodiment.

Processor **116** may include a microprocessor, a microcontroller, control logic, a multi-core processor, or the like. Memory **117** may include a variety of memories, such as a volatile memory **117***a* (e.g., a RAM), a nonvolatile memory **117***b* (e.g., a disk, FLASH, or the like). Different implementations of tissue oximetry device **100** may include any number of the listed components, in any combination or configuration, and may also include other components not shown.

Power source **127** can be a battery, such as a disposable battery. Disposable batteries are discarded after their stored charge is expended. Some disposable battery chemistry technologies include alkaline, zinc carbon, or silver oxide. The battery has sufficient stored charged to allow use of the handheld device for several hours. After use, the handheld unit is discarded.

In other implementations, the battery can also be rechargeable where the battery can be recharged multiple times after the stored charge is expended. Some rechargeable battery chemistry technologies include nickel cadmium (NiCd), nickel metal hydride (NiMH), lithium ion (Li-ion), and zinc air. The battery can be recharged, for example, via an AC adapter with cord that connects to the handheld unit. The circuitry in the handheld unit can include a recharger circuit (not shown). Batteries with rechargeable battery chemistry may be sometimes used as disposable batteries, where the batteries are not recharged but disposed of after use.

Stored Simulated Reflectance Curves

According to a specific embodiment, memory **117** stores a number of Monte Carlo-simulated reflectance curves **315** ("simulated reflectance curves"), which may be generated by a computer for subsequent storage in the memory. Each of the simulated reflectance curves **315** represents a simulation of light (e.g., near infrared light) emitted from one or more simulated light sources into simulated tissue and reflected from the simulated tissue into one or more simulated detectors. Simulated reflectance curves **315** are for a specific configuration of simulated light sources and simulated detectors, such as the configuration of light sources **120** and detectors **125** in tissue oximetry probes **115**, **115'**, or the like. Therefore, simulated reflectance curves **315** model light emitted from, and collected by, tissue oximetry device **100**. Further, each of the simulated reflectance curves **315** represents a unique real tissue condition, such as specific tissue absorption and tissue scattering values that relate to particular concentrations of tissue chromophores and densities of tissue scatterers. The number of simulated reflectance curves stored in memory **117** may be relatively large and can represent nearly all, if not all, practical combinations of optical properties and tissue properties that may be present in real tissue that is analyzed for viability by tissue oximetry device **100**. While memory **117** is described herein as storing Monte Carlo-simulated reflectance curves, memory **117** may store simulated reflectance curves generated by methods other than Monte Carlo methods, such as using the diffusion approximation.

FIG. **4** is an example graph of a reflectance curve, which may be for a specific configuration of light sources **120** and detectors **125**, such as one of the configurations light sources and detectors of tissue oximetry probes **115**, **115'**, or the like. The horizontal axis of the graph represents the distances between light sources **120** and detectors **125** (i.e., source-detector distances). If the distances between light sources **120** and detectors **125** are appropriately chosen, and the simulated reflectance curve is a simulations for light sources **120** and detectors **125**, then the lateral spacings between the data points in the simulated reflectance curve will be relatively uniform. Such relatively uniform spacings can be seen in the simulated reflectance curve in FIG. **4**. The vertical axis of the graph represents the simulated reflectance of light that reflects from tissue and is detected by detectors **125**. As shown by the simulated reflectance curve, the reflectance that reaches detectors **125** varies with the distance between light sources **120** and detectors **125**.

According to one implementation, memory **117** stores a select number of points for each of the simulated reflectance curves **315** and might not store the entirety of the simulated reflectance curves. The number of points stored for each of simulated reflectance curves **315** may match the number of

source-detector pairs. For example, if tissue oximetry probe **115** includes two light sources **120***a* and **120***c* and includes eight detectors **125***a*-**125***h*, then tissue oximetry probe **100** includes sixteen source-detector pairs, and memory **117** may thus store sixteen select data points for each of the simulated reflectance curves, where stored data points are for the specific source-detectors distances (i.e., distances between the light sources and the detectors).

Thus, the simulated reflectance curve database stored in memory **117** might be sized 16×3×5850 where sixteen points are stored per curve for three different wavelengths that may be generated and emitted by each light source **210** and wherein there are a total of 5850 curves spanning the optical property ranges. Alternatively, the simulated reflectance curve database stored in memory **117** might be sized 16×4×5850 wherein sixteen points are stored per curve for four different wavelengths that may be generated and emitted by each light source and wherein there are a total of 5850 curves spanning the optical property ranges. The 5850 curves originate, for example, from a matrix of 39 absorption coefficients μ_s' values and 150 absorption coefficient μ_a values. The μ_s' values might range from 5:5:24 centimeter^{-1} (μ_s' depends on the value for g). The μ_a values might range from 0.01:0.01:1.5. It will be understood the foregoing described ranges are example ranges and the number source-detectors pairs, the number of wavelengths generated by each light source, and the number of simulated reflectance curves may be smaller or larger.

Tissue Analysis

FIG. **5**A is a high-level flow diagram of a method for determining the optical properties of tissue (e.g., real tissue) by tissue oximetry device **100** where the tissue oximetry device uses reflectance data and simulated reflectance curves **315** to determine the optical properties. The optical properties may include the absorption coefficient μ_a and the scattering coefficients μ_s of the tissue. A further method for conversion of the absorption coefficient μ_a and the scattering coefficients of the tissue μ_s to oxygen saturation values for tissue is described in further detail below. The high-level flow diagram represents one example embodiment. Steps may be added to, removed from, or combined in the high-level flow diagram without deviating from the scope of the embodiment.

At **500**, tissue oximetry device **100** emits light (e.g., near infrared light) from one of the light sources **120**, such as light source **120***a* into tissue. The tissue oximetry device is generally in contact with the tissue when the light is emitted from the light source. After the emitted light reflects from the tissue, detectors **125** detect a portion this light, step **505**, and generate reflectance data points for the tissue, step **510**. Steps **500**, **505**, and **510** may be repeated for multiple wavelengths of light (e.g., red, near infrared light, or both) and for one or more other light sources, such as light source **120***c*. The reflectance data points for a single wavelength might include sixteen reflectance data points if, for example, tissue oximetry probe **115** has sixteen source-detectors distances. The reflectance data points are sometimes referred to as an N-vector of the reflectance data points.

At **515**, the reflectance data points (e.g., raw reflectance data points) are corrected for gain of the source-detector pairs. During calibration of the source-detector pairs, gain corrections are generated for the source-detector pairs and are stored in memory **117**. Generation of the gain corrections are described in further detail below.

At **520**, processor **116** fits (e.g., via a sum of squares error calculation) the reflectance data points to the simulated reflectance curves **315** to determine the particular reflectance data curve that best fits (i.e., has the lowest fit error) the reflectance data points. According to one specific implementation, a relatively small set of simulated reflectance curves that are a "coarse" grid of the database of the simulated reflectance curves is selected and utilized for fitting step **520**. For example, given **39** scattering coefficient μ_s' values and 150 absorption coefficient μ_a values, a coarse grid of simulated reflectance curves might be determined by processor **116** by taking every 5th scattering coefficient μ_s' value and every 8th absorption coefficients μ_a for a total of 40 simulated reflectance curves in the coarse grid. It will be understood that the foregoing specific values are for an example embodiment and that coarse grids of other sizes might be utilized by processor **116**. The result of fitting the reflectance data points to the coarse grid is a coordinate in the coarse grid $(\mu_a, \lambda_s')_{coarse}$ of the best fitting simulated reflectance curve.

At **525**, the particular simulated reflectance curve from the coarse grid having the lowest fit error is utilized by processor **116** to define a "fine" grid of simulated reflectance curves where the simulated reflectance curves in the fine grid are around the simulated reflectance curve from the coarse grid having the lowest fit error.

That is, the fine grid is a defined size, with the lowest error simulated reflectance curve from the coarse grid defining the center of the fine grid. The fine grid may have the same number of simulated reflectance curves as the coarse grid or it may have more or fewer simulated reflectance curves. The fine grid is substantially fine so as to provide a sufficient number of points to determine a peak surface array of nearby absorption coefficient μ_a values and scattering coefficient μ_s' values, step **530**, in the fine grid. Specifically, a threshold may be set by processor **116** utilizing the lowest error value from the coarse grid plus a specified offset. The positions of the scattering coefficient μ_s' and the absorption coefficient μ_a on the fine grid that have errors below the threshold may all be identified for use in determining the peak surface array for further determining the scattering coefficient μ_s' and the absorption coefficient μ_a for the reflectance data. Specifically, an error fit is made for the peak to determine the absorption coefficient μ_a and the scattering coefficient μ_s' values at the peak. A weighted average (e.g., a centroid calculation) of the absorption coefficient μ_a and the scattering coefficient μ_s' values at the peak may be utilized by the tissue oximetry device for the determination of the absorption coefficient μ_a and the scattering coefficient μ_s' values for the reflectance data points for the tissue, step **540**.

Weights for the absorption coefficient μ_a and the scattering coefficient μ_s' values for the weighted average may be determined by processor **116** as the threshold minus the fine grid error. Because points on the fine grid are selected with errors below the threshold, this gives positive weights. The weighted calculation of the weighted average (e.g., centroid calculation) renders the predicted scattering coefficient μ_s' and absorption coefficient μ_a (i.e., $(\mu_a,\mu_s')_{fine}$) for the reflectance data points for the tissue. Other methods may be utilized by the tissue oximetry device, such as fitting with one or more of a variety of non-linear least squares to determine the true minimum error peak for the scattering coefficient us.

According to one implementation, processor **116** calculates the log of the reflectance data points and the simulated reflectance curves, and divides each log by the square root of the source-detector distances (e.g., in centimeters). These log values divided by the square root of the of the source-detector distances may be utilized by processor **116** for the reflectance data points and the simulated reflectance curves

in the foregoing described steps (e.g., steps **515**, **520**, **525**, and **530**) to improve the fit of the reflectance data points to the simulated reflectance curves.

According to another implementation, the offset is set essentially to zero, which effectively gives an offset of the difference between the coarse grid minimum and the fine grid minimum. The method described above with respect to FIG. **5**A relies on minimum fit error from the coarse grid, so the true minimum error on the fine grid is typically lower. Ideally, the threshold is determined from the lowest error on the fine grid, which would typically require additional computation by the processor.

The following is a further detailed description for finding the particular simulated reflectance curve that best fits the reflectance data points in the fine grid according to one implementation. FIG. **5**B is a high-level flow diagram of a method for finding the particular simulated reflectance curve that best fits the reflectance data points in the fine grid according to one implementation. The high-level flow diagram represents one example embodiment. Steps may be added to, removed from, or combined in the high-level flow diagram without deviating from the scope of the embodiment.

Subsequent to determining the particular simulated reflectance curve $(\mu_a,\mu_s')_{coarse}$ from the coarse grid that best fits the reflectance data points at step **525**, processor **116** computes an error surface in a region about $(\mu_a,\mu_s')_{coarse}$ in the full simulated reflectance curve database (i.e., 16×3×5850 (μ_a,μ_s') database) of simulated reflectance curves, step **550**. The error surface is denoted as: $err(\mu_a,\mu_s')$. Thereafter, processor **116** locates the minimum error value in $err(\mu_a,\mu_s')$, which is referred to as err_{min}, step **555**. Processor **116** then generates a peak surface array from $err(\mu_a,\mu_s')$ that is denoted by $pksurf(\mu_a,\mu_s')=k+err_{min}-err(\mu_a,\mu_s')$ if the peak surface is greater than zero, or $pksurf(\mu_a,\mu_s')=k+err_{min}-err(\mu_a,\mu_s')=0$ if the peak surface is less than or equal to zero, step **560**. In the expression k is chosen from a peak at the minimum point of $err(\mu_a,\mu_s')$ with a width above zero of approximately ten elements. The center-of-mass (i.e., the centroid calculation) of the peak in $pksurf(\mu_a,\mu_s')$ uses the heights of the points as weights, step **565**. The position of the center-of-mass is the interpolated result for the absorption coefficient μ_a and the scattering coefficient μ_s' for the reflectance data points for the tissue.

The method described above with respect to FIGS. **5**A and **5**B for determining the absorption coefficient μ_a and the scattering coefficient μ_s' for reflectance data points for tissue may be repeated for each of the wavelengths (e.g., 3 or 4 wavelengths) generated by each of light sources **120**.

Oxygen Saturation Determination

According to a first implementation, processor **116** determines the oxygen saturation for tissue that is probed by tissue oximetry device **100** by utilizing the absorption coefficients μ_a (e.g., 3 or 4 absorption coefficients μ_a) that are determined (as described above) for the 3 or 4 wavelengths of light that are generated by each light source **120**. According to a first implementation, a look-up table of oxygen saturation values is generated for finding the best fit of the absorption coefficients μ_a to the oxygen saturation. The look-up table may be generated by assuming a range of likely total hemoglobin, melanin, and oxygen saturation values and calculating μ_a for each of these scenarios. Then, the absorption coefficient μ_a points are converted to a unit vector by dividing by a norm of the unit vector to reduce systematic error and only depend on relative shape of curve. Then the unit vector is compared to the look-up table to find the best fit, which gives the oxygen saturation.

According to a second implementation, processor **116** determines the oxygen saturation for the tissue by calculating the net analyte signal (NAS) of deoxygenated hemoglobin and oxygenated hemoglobin. The NAS is defined as the portion of the spectrum that is orthogonal to the other spectral components in the system. For example, the NAS of deoxygenated hemoglobin is the portion of the spectrum that is orthogonal to oxygenated hemoglobin spectrum and melanin spectrum. The concentrations of deoxygenated and oxygenated hemoglobin can then be calculated by vector multiplying the respective NAS and dividing by a norm of the NAS squared. Oxygen saturation is then readily calculated as the concentration of oxygenated hemoglobin divided by the sum of oxygenated hemoglobin and deoxygenated hemoglobin. Anal. Chem. 58:1167-1172 (1986) by Lorber is incorporated by reference herein and provides a framework for a further detailed understanding of the second implementation for determining the oxygen saturation for the tissue.

According to one embodiment of tissue oximetry device **100**, the reflectance data is generated by detectors **125** at 30 Hertz, and oxygen saturation values are calculated at approximately 3 Hertz. A running average of determined oxygen saturation values (e.g., at least three oxygen saturation values) may be displayed on display **112**, which might have an update rate of 1 Hertz.

Optical Properties

As described briefly above, each simulated reflectance curve **315** that is stored in memory **117** represents unique optical properties of tissue. More specifically, the unique shapes of the simulated reflectance curves, for a given wavelength, represent unique values of the optical properties of tissue, namely the scattering coefficient GO, the absorption coefficient (μ_a), the anisotropy of the tissue (g), and index of refraction of the tissue from which the tissue properties may be determined.

The reflectance detected by detectors **125** for relatively small source-to-detector distances is primarily dependent on the reduced scattering coefficient, μ_s'. The reduced scattering coefficient is a "lumped" property that incorporates the scattering coefficient μ_s and the anisotropy g of the tissue where $\mu_s'=\mu_s(1-g)$, and is used to describe the diffusion of photons in a random walk of many steps of size of $1/\mu_s$ where each step involves isotropic scattering. Such a description is equivalent to a description of photon movement using many small steps $1/\mu_s$ which each involve only a partial deflection angle if there are many scattering events before an absorption event, i.e., $\mu_a<<\mu_s'$.

In contrast, the reflectance that is detected by detectors **125** for relatively large source-detector distances is primarily dependent on the effective absorption coefficient μ_{eff}, which is defined as $\sqrt{3\mu_a(\mu_a+\mu_s')}$, which is a function of both μ_a and μ_s'.

Thus, by measuring reflectance at relatively small source-detector distances (e.g., D**1** between light source **120***a* and detector **125***e* and D**9** between light source **120***c* and detector **125***a*) and relatively large source-detector distances (e.g., D**5** between light source **120***a* and detector **125***a* and D**10** between light source **120***c* and detector **125***e*), both μ_a and μ_s' can be independently determined from one another. The optical properties of the tissue can in turn provide sufficient information for the calculation of oxygenated hemoglobin and deoxygenated hemoglobin concentrations and hence the oxygen saturation of the tissue.

Iterative Fit for Data Collection Optimization.

FIG. **6** is a high-level flow diagram of another method for determining the optical properties of tissue by tissue oximetry device **100**. The high-level flow diagram represents one example embodiment. Steps may be added to, removed from, or combined in the high-level flow diagram without deviating from the scope of the embodiment.

At **600**, tissue oximetry device **100** emits light (e.g., near infrared light) from one of the light sources, such as light source **120***a* into tissue. After the emitted light reflects from the tissue, detectors **125** detect the light, step **605**, and generate reflectance data for the tissue, step **610**. Steps **600**, **605**, and **610** may be repeated for multiple wavelengths of light and for one or more other light sources, such as light source **120***c*. At **615**, tissue oximetry device **100** fits the reflectance data to simulated reflectance curves **315** and determines the simulated reflectance curve to which the reflectance data has the best fit. Thereafter, tissue oximetry device **100** determines the optical properties (e.g., μ_a, and μ_s') for the tissue based on the optical properties of the simulated reflectance curve that best fits the reflectance data, step **620**.

At **625** tissue oximetry device **100** determines the mean free path of the light in the tissue from the optical properties (e.g., $mfp=1/(\mu_a+\mu_s')$) determined at step **620**. Specifically, the mean free path can be determined from the optical properties obtained from a cumulative reflectance curve that includes the reflectance data for all of the source-detector pairs (e.g., pair 1: light source **120***a*-detector **125***e*; pair 2: light source **120***a*-detector **125***f*; pair 3: light source **120***a*-detector **125***g*; pair 4: light source **120***a*-detector **125***h*; pair 5: light source **120***a*-detector **125***a*; pair 6: light source **120***a*-detector **125***b*; pair 7: light source **120***a*-detector **125***c*; pair 8: light source **120***a*-detector **125***d*; . . . pair 9: light source **120***c*-detector **125***e*, pair **10**: light source **120***b*-detector **125***f* . . . and others.).

At **630**, tissue oximetry device **100** determines whether the mean free path calculated for a given region of the tissue is longer than two times the shortest source-to-detector distance (e.g., D**1** between light source **120***a* and detector **125***e*, and D**9** between light source **120***c* and detector **125***a*). If the mean free path is longer than two times the shortest source-to-detector distance, then the collected reflectance data is re-fitted to the simulated reflectance curves (i.e., reanalyzed) without utilizing the reflectance data collected from the detectors for the source-to-detector pairs (e.g., pair 1: light source **120***a*-detector **125***e* and pair 9 light source **120***c*-detector **125***a*) having the shortest source-to-detector distance. For example, steps **615-630** are repeated without use of the reflectance data from detector **125***e* with light source **120***a* acting as the source for detector **125***e*, and without use of the reflectance data from detector **125***a* with light source **120***c* acting as the source for detector **125***a*. The process of calculating the mean free path and discarding the reflectance data for one or more source-detector pairs may be repeated until no source-detector pairs that contribute reflectance data to the fit have a source-to-detector distance shorter than one half of the calculated mean free path. Thereafter, oxygen saturation is determined from the best fitting simulated reflectance curve and reported by tissue oximetry device **110**, such as on display **112**, step **635**.

Light that is emitted from one of the light sources **120** into tissue and that travels less than half of the mean free path is substantially non-diffusely reflected. The re-emission distance for this light is strongly dependent on the tissue phase function and the local tissue composition. Therefore, using the reflectance data for this light tends to result in a less accurate determination of the optical properties and tissue properties as compared with the reflectance data for light that has undergone multiple scattering events.

Data Weighting

Detectors **125** that are positioned at increasing distances from light sources **120** receive decreasing amounts of reflectance from tissue. Therefore, the reflectance data generated by detectors **125** having relatively short source-to-detector distances (e.g., D**1**) tends to exhibit intrinsically lower noise compared to reflectance data generated by detectors having relatively long source-to-detector distances (e.g., D**5** and D**10**). Fit algorithms may therefore preferentially fit the simulated reflectance curves to the reflectance data that is generated by detectors **125** having relatively short source-to-detectors distances (e.g., source-to-detector distances less than or equal to the average distance between the light sources and the detectors) more tightly than reflectance data that is generated by detectors having relatively long source-to-detector distances (e.g., source-to-detector distances greater than the average distance). For relatively accurate determination of the optical properties from the reflectance data, this distance-proportional skew may be undesirable and may be corrected by weighting the reflectance data as described immediately below.

FIG. **7** is a high-level flow diagram of a method for weighting reflectance data generated by select detectors **125**. The high-level flow diagram represents one example embodiment. Steps may be added to, removed from, or combined in the high-level flow diagram without deviating from the scope of the embodiment.

At **700**, tissue oximetry device **100** emits light from one of the light sources, such as light source **120***a* into tissue. After the emitted light reflects from the tissue, detectors **125** detect the light, step **705**, and generate reflectance data for the tissue, step **710**. Steps **700**, **705**, and **710** may be repeated for multiple wavelengths of light and for one or more other light sources, such as light source **120***c*. At **715**, tissue oximetry device **100** fits a first portion of the reflectance data to the simulated reflectance curves. The first portion of the reflectance data is generated by a first portion of detectors that are less than a threshold distance from the light source. The threshold distance may be the average distances (e.g., approximate mid-range distance) between the light sources and the detectors. At **720**, reflectance data for a second portion of the reflectance data is fitted to the simulated reflectance curves. The second portion of reflectance data is generated by the first portion of the detectors and another detector that is at the next largest source-to-detector distance from the source compared to the threshold distance. For example, if the first portion of detectors includes detectors **125***c*, **125***d*, **125***e*, and **125***f*, then the detector that is at the next largest source-to-detector distance is detector **125***g* (e.g., closer to light source **120***a* than detector **125***c*, see FIGS. **2**A and **2**B).

At **725**, the fit generated at step **715** is compared to the fit generated at step **720** to determine whether the fit generated at step **720** is better than the fit generated at **715**. As will be understood by those of skill in the art, a "closeness" of a fit of data to a curve is quantifiable based on a variety of parameters, and the closeness of fits are directly comparable to determine the data having a closer fit (closer fit) to a curve. As will be further understood, a closer fit is sometimes also referred to as a better fit or a tighter fit. If the fit generated at step **720** is better than the fit generated at step **715**, then steps **720** and **725** are repeated with reflectance data that is generated by detectors that include an additional detector (according to the example being considered, detector **125***c*) that is positioned at a next increased source-to-

detector distance from the source. Alternatively, if the fit generated at step **720** is not better than the fit generated at step **715**, then the reflectance data for detectors **125** that are positioned at source-to-detector distances that are greater than the threshold distance are not used in the fit. Thereafter, tissue oximetry device **100** uses the fit generated at **715** or step **720** (if better than the fit determined at step **715**) to determine the optical properties and the oxygen saturation of the tissue, step **730**. Thereafter, oxygen saturation is reported by tissue oximetry device **110**, such as on display **112**, step **735**.

According to an alternative embodiment, if the fit generated at step **720** is not better than the fit generated at step **715**, then the reflectance data are weighted by a weighting factor for detectors that have source-to-detector distances that are greater than the threshold distance so that this weighted reflectance data has a decreased influence on the fit. Reflectance data that is not used in a fit may be considered as having a zero weight and may be associated with reflectance from tissue below the tissue layer of interest. Reflectance from tissue below the tissue layer of interest is said to exhibit a characteristic kink in the reflectance curve that indicates this particular reflectance.

It is noted that curve-fitting algorithms that fit the reflectance data to the simulated reflectance curves may take into account the amount of uncertainty of the reflectance data as well as the absolute location of the reflectance data. Uncertainty in the reflectance data corresponds to the amount of noise from the generation of the reflectance data by one of the detectors, and the amount of noise can scale as the square root of the magnitude of the reflectance data.

According to a further embodiment, tissue oximetry device **100** iteratively weights the reflectance data based on the amount of noise associated with the measurements of the reflectance data. Specifically, the reflectance data generated by detectors having relatively large source-to-detector distances generally have greater a greater signal-to-noise ratio compared to the reflectance data generated by detector having relatively short source-to-detector distances. Weighting the reflectance data generated by detectors having relatively large source-to-detector distances allows for this data to contribute to the fit substantially equally to other reflectance data.

Calibration

According to one embodiment, tissue oximetry device **100** is calibrated utilizing a number (e.g., three to thirty) of tissue phantoms that have known optical properties. Tissue oximetry device **100** may be used to probe the tissue phantoms and collect reflectance data for the tissue phantoms. The reflectance data for each tissue phantom may be fitted to simulated reflectance curves **315**. The reflectance data generated for each tissue phantom should fit a simulated reflectance curve, which has the same optical properties as the tissue phantom. If the optical properties of the simulated reflectance curve to which the reflectance data is fitted does not match the optical properties of the tissue phantom, then a calibration function may be generated by tissue oximetry device **100** to improve the fit. The calibration function for each of the tissue phantoms and matched simulated reflectance curves should substantially match. One or more of the calibration functions or an average of the calibration functions may be stored in memory **117**. The one or more calibration functions may be applied to reflectance data generated for real tissue that is probed by tissue oximetry device **100** so that the reflectance data for the real tissue will fit to one of the simulated reflectance curves that has optical properties that are a substantially accurate match to the optical properties of the real tissue. Thereafter, the optical properties for the matched simulated reflectance curve may be used to calculate and report the oxygenation saturation of the real tissue.

Methods described herein for matching reflectance data to a number of Monte Carlo-simulated reflectance curves provides for relatively fast and accurate determination of the optical properties of real tissue probed by the tissue oximetry device. Speed in determining optical properties of tissue is an important consideration in the design of intraoperative probes compared to postoperative probes. Further, the Monte Carlo methods described herein allow for robust calibration methods that in-turn allow for the generation of absolute optical properties as compared with relative optical properties. Reporting absolute optical properties, as opposed to relative optical properties, is relatively important for intra-operative probes as compared with post-operative probes.

This description of the invention has been presented for the purposes of illustration and description. It is not intended to be exhaustive or to limit the invention to the precise form described, and many modifications and variations are possible in light of the teaching above. The embodiments were chosen and described in order to best explain the principles of the invention and its practical applications. This description will enable others skilled in the art to best utilize and practice the invention in various embodiments and with various modifications as are suited to a particular use. The scope of the invention is defined by the following claims.

The invention claimed is:

1. A method comprising:

storing in nonvolatile memory of a tissue oximeter device simulated reflectance curves, wherein the nonvolatile memory retains the simulated reflectance curves even after the device is powered off;

causing light to emit from at least one source of the tissue oximeter device into a tissue to be measured;

receiving at least one detector of the tissue oximeter device light reflected from the tissue in response to the emitted light; and

based on the reflected light and the simulated reflectance curves stored in the nonvolatile memory, calculating an oxygen saturation value for the tissue, wherein a processor of the tissue oximeter device is configured to:

determine a plurality of digital reflectance data points for the reflected light;

retrieve the simulated reflectance curves from the nonvolatile memory, wherein the simulated reflectance curves were previously determined, before the processor determines the digital reflectance data points;

based on the digital reflectance data points, determine a first subset of the simulated reflectance curves based on a coarse grid, wherein each curve in the first subset is separated by an interval from another curve of the first subset;

calculate a closest fitting of the digital reflectance data points to a closest fit curve of the first subset of simulated reflectance curves;

based on the digital reflectance data points, determine a second subset of the simulated reflectance curves based on a fine grid; and

using the closest fit curve and second subset of simulated reflectance curves, calculate a set of absorption coefficients and a set of scattering coefficients for the reflectance data points, wherein the set of absorption

coefficients and the set of scattering coefficients are used in the calculating an oxygen saturation value for the tissue,

wherein the processor of the tissue oximeter device is not used to calculate the simulated reflectance curves,

the tissue oximeter device comprises

a plurality of sources, the sources are arranged along a line, and

a plurality of detectors, wherein there are an equal number of detectors on either side of this line,

a curve of the simulated reflectance curves comprises a first axis comprising a source-detector separation distance and a second axis comprising reflectance intensity,

the curve comprises a first curve point having a first reflectance intensity at a first source-detector separation distance, and a second curve point having a second reflectance intensity at a second source-detector separation distance,

for the first curve point, the first reflectance intensity is greater than the second reflectance intensity, and the first source-detector separation distance is less than the second source-detector separation distance, and

for the second curve point, the second reflectance intensity is less than the first reflectance intensity, and the second source-detector separation distance is greater than the first source-detector separation distance.

2. The method of claim **1** the tissue oximeter device comprises a housing to enclose the processor,

a volatile memory, coupled to the processor, wherein the volatile memory does not retain its contents after the device is powered off, and

a battery, coupled to the processor and the volatile and nonvolatile memories.

3. The method of claim **1** wherein the curve comprises a third curve point having a third reflectance intensity at a third source-detector separation distance, and a fourth curve point having a fourth reflectance intensity at a fourth source-detector separation distance.

4. The method of claim **3** wherein for the third curve point, the third reflectance intensity is greater than the fourth reflectance intensity, and the third source-detector separation distance is less than the fourth source-detector separation distance.

5. The method of claim **4** wherein for the fourth curve point, the fourth reflectance intensity is less than the third reflectance intensity, and the fourth source-detector separation distance is greater than the third source-detector separation distance.

6. The method of claim **1** wherein a first slope of a line through the first and second curve points is negative.

7. The method of claim **3** wherein a first slope of a line through the first and second curve points is negative.

8. The method of claim **3** wherein a second slope of a line through the third and fourth curve points is negative.

9. The method of claim **3** wherein a first slope of a line through the first and second curve points is negative, a second slope of a line through the third and fourth curve points is negative, and the second slope is less negative than the first slope.

10. The method of claim **4** wherein a first slope of a line through the first and second curve points is negative.

11. The method of claim **4** wherein a second slope of a line through the third and fourth curve points is negative.

12. The method of claim **4** wherein a first slope of a line through the first and second curve points is negative, a second slope of a line through the third and fourth curve points is negative, and the second slope is less negative than the first slope.

13. The method of claim **5** wherein a first slope of a line through the first and second curve points is negative.

14. The method of claim **5** wherein a second slope of a line through the third and fourth curve points is negative.

15. The method of claim **5** wherein a first slope of a line through the first and second curve points is negative, a second slope of a line through the third and fourth curve points is negative, and the second slope is less negative than the first slope.

16. A method comprising:

storing in nonvolatile memory of a tissue oximeter device simulated reflectance curves, wherein the nonvolatile memory retains the simulated reflectance curves even after the device is powered off;

causing light to emit from at least one source of the tissue oximeter device into a tissue to be measured;

receiving at least one detector of the tissue oximeter device light reflected from the tissue in response to the emitted light; and

based on the reflected light and the simulated reflectance curves stored in the nonvolatile memory, calculating an oxygen saturation value for the tissue, wherein a processor of the tissue oximeter device is configured to:

determine a plurality of digital reflectance data points for the reflected light;

retrieve the simulated reflectance curves from the nonvolatile memory, wherein the simulated reflectance curves were previously determined, before the processor determines the digital reflectance data points;

based on the digital reflectance data points, determine a first subset of the simulated reflectance curves based on a coarse grid, wherein each curve in the first subset is separated by an interval from another curve of the first subset;

calculate a closest fitting of the digital reflectance data points to a closest fit curve of the first subset of simulated reflectance curves;

based on the digital reflectance data points, determine a second subset of the simulated reflectance curves based on a fine grid; and

using the closest fit curve and second subset of simulated reflectance curves, calculate a set of absorption coefficients and a set of scattering coefficients for the reflectance data points, wherein the set of absorption coefficients and the set of scattering coefficients are used in the calculating an oxygen saturation value for the tissue,

wherein the processor of the tissue oximeter device is not used to calculate the simulated reflectance curves,

the tissue oximeter device comprises

a plurality of sources, the sources are arranged along a line, and

a plurality of detectors, wherein first and second pluralities of the plurality of detectors are positioned on either side of this line,

a curve of the simulated reflectance curves comprises a first axis comprising a source-detector separation distance and a second axis comprising reflectance intensity,

the curve comprises a first curve point having a first reflectance intensity at a first source-detector separation distance, and a second curve point having a second reflectance intensity at a second source-detector separation distance,

for the first curve point, the first reflectance intensity is greater than the second reflectance intensity, and the first source-detector separation distance is less than the second source-detector separation distance, and

for the second curve point, the second reflectance intensity is less than the first reflectance intensity, and the second source-detector separation distance is greater than the first source-detector separation distance.

17. The method of claim **16** the tissue oximeter device comprises a housing to enclose the processor,

a volatile memory, coupled to the processor, wherein the volatile memory does not retain its contents after the device is powered off, and

a battery, coupled to the processor and the volatile and nonvolatile memories.

18. The method of claim **17** wherein the curve comprises a third curve point having a third reflectance intensity at a third source-detector separation distance, and a fourth curve point having a fourth reflectance intensity at a fourth source-detector separation distance.

19. The method of claim **18** wherein for the third curve point, the third reflectance intensity is greater than the fourth reflectance intensity, and the third source-detector separation distance is less than the fourth source-detector separation distance.

20. The method of claim **19** wherein for the fourth curve point, the fourth reflectance intensity is less than the third reflectance intensity, and the fourth source-detector separation distance is greater than the third source-detector separation distance.

* * * * *